

**GROWTH AND CHARACTERIZATION
OF GALLIUM NITRIDE FILMS ON
POROUS SILICON SUBSTRATE**

**MUHAMMAD ESMED ALIF BIN
SAMSUDIN**

UNIVERSITI SAINS MALAYSIA

2016

**GROWTH AND CHARACTERIZATION
OF GALLIUM NITRIDE FILMS ON
POROUS SILICON SUBSTRATE**

by

**MUHAMMAD ESMED ALIF BIN
SAMSUDIN**

**Thesis submitted in fulfilment of the requirements for the degree of
Master of Science**

MARCH 2016

ACKNOWLEDGEMENT

In the name of Allah, the beneficent the merciful.

Alhamdulillah, all thanks to The Almighty with His grace, I managed to complete this dissertation successfully. First and foremost, I would like express my deepest gratitude to my supervisor, Dr. Norzaini Zainal, for her precious guidance and persistence support throughout my research works. With her valuable knowledge, many unexpected circumstances which came across during the research progress are able to be solved. Moreover, thanks to her again for giving me a chance to be a part of her nitrides research team and appointing me as her research assistant, which indirectly gives me a precious experienced throughout my time as a master student.

On this occasion, I also would like to thank to Malaysian government for MyBrain15 scholarship and Majlis Amanah Rakyat (MARA) that provides me with financial support during my study. Furthermore, I wish to thank to my beloved colleagues, Ikram, Azharul, Alvin, Waheeda, and Ezzah for being helpful during my hard and ease time. All the precious moments that we get through together are forever remembered. Also not to be forgotten to Prof. Zainuriah Hassan, who acts as my co-authors in several journals and Dr-to-be Rosfariza Radzali for her great assistance in porous experiments.

On the other hand, I would like to acknowledge all N.O.R staffs for their kindness and technical supports, especially for Mr. Anas Ahmad, Mdm Ee Bee Choo, Mr. Yushamdan and Mr. Jamil. Last but not least, I dedicated this thesis for my beloved parents, Haji Samsudin and Pn Jaliah, for their blessing and dua'a. Not to be forgotten my lovely siblings for their encouragement and support. Without them, this work could not be able to finish. I love you all.

TABLE OF CONTENTS

	Page
ACKNOWLEDGEMENT	ii
TABLE OF CONTENTS	iii
LIST OF TABLES	ix
LIST OF FIGURES	xi
LIST OF SYMBOLS	xviii
LIST OF ABBREVIATIONS	xix
ABSTRAK	xxi
ABSTRACT	xxiii
CHAPTER 1: INTRODUCTION TO GaN SEMICONDUCTOR	1
CHAPTER 2: BASIC PROPERTIES AND LITERATURE REVIEW OF GaN	6
2.1 Introduction to GaN material.....	6
2.1.1 Basic crystal structure of GaN material.....	6
2.2 Growing GaN on Si substrate and its general issues.....	9
2.2.1. Progress of GaN growth onto Si substrate.....	9
2.2.2 Si substrate orientation: Si (111) versus Si (100).....	11
2.2.3 Issue on growing GaN on Si substrate.....	12
2.3 Role of buffer layer in GaN growth on Si substrate.....	14
2.4 Introduction of porous Si and its fabrication.....	17
2.5 Growth of GaN on porous Si/Si substrate.....	19

2.5.1. Main role of porous Si/Si substrate for GaN growth.....	20
2.5.2 Progress in the growth of GaN on porous Si/Si substrate.....	21
2.5.3 Growth of GaN on porous Si/Si substrate using cost-effective technique.....	22
2.6 Annealing treatment as a strategy to improve GaN properties.....	23
2.7 Summary.	24

CHAPTER 3: SAMPLE PREPARATION AND EXPERIMENTAL PROCEDURES.....25

3.1 Preparation of porous Si substrates for GaN growth.....	26
3.1.1 Preparation of chemical solutions for Si substrate cleaning.....	26
3.1.2 Fabrication of porous Si via electrochemical etching.....	27
3.2 Growth of GaN layer using RF sputtering and e-beam evaporator.....	30
3.2.1 Basic operation of radio-frequency (RF) sputtering.....	30
3.2.2 Preparation of buffer layers by radio-frequency (RF) sputtering.....	31
3.2.3 Growth of GaN layers on nitrides buffer layers and porous Si substrates by RF sputtering.....	33
3.2.4 Growth of GaN layer using e-beam evaporator.....	34
3.2.5. Growth of GaN layers on nitrides buffer layer and porous Si substrate by e-beam evaporator.....	36
3.2.6 Post-annealing treatment on GaN layer.....	37
3.3 Characterization measurements on samples.....	39
3.3.1 Surface morphology analysis.....	39
3.3.1.1 Field emission scanning electron microscopy (FESEM) measurement.....	40
3.3.1.2 Atomic Force Microscopy (AFM) measurement.....	42
3.3.2 Crystallography analysis.....	45

3.3.2.1 High resolution X-ray diffraction (HR-XRD) measurement.....	46
3.3.2.1.1 XRD 2θ - ω scan (phase analysis measurement).....	47
3.3.2.1.2 Omega (ω) scan (rocking curve measurements).....	49
3.3.2.2 X-ray photoelectron spectroscopy measurement.....	51
3.3.3 Optical analysis.....	53
3.3.3.1 Photoluminescence (PL) measurement.....	54
3.3.3.2 Raman spectroscopy measurement.....	55
3.4 Summary.....	57

CHAPTER 4: PREPARATION OF POROUS Si (100) SUBSTRATE BY ELECTROCHEMICAL ETCHING.....58

4.1 Role of ethanol in improving porosity of Si (100) substrate.....	58
4.1.1 Effect of different concentration of ethanol in the mixture of HF and ethanol on porosity of Si (100)	58
4.1.2 Effect of different current density on porosity of Si (100).....	60
4.1.3 Effect of different etching time on porosity of Si (100).....	62
4.2 Role of hydrogen peroxide in improving the porosity of Si.....	67
4.2.1 Effect of different concentration of H ₂ O ₂ in the mixture of HF, ethanol and H ₂ O ₂ on porosity of Si (100).....	67
4.2.2 Effect of different etching time in the mixture of HF, ethanol and H ₂ O ₂ on porosity of Si (100).....	69
4.3 Role of dimethylformamide in improving the porosity of Si.....	70
4.3.1 Effect of different ratio of DMF in the mixture of HF on porosity of Si (100).....	71
4.3.2 Effect of etching time in the mixture of HF and DMF on porosity of Si (100).....	72
4.4 Summary.....	74

CHAPTER 5: GROWTH OF GaN LAYERS ON Si, AlN/Si, TiN/Si AND POROUS Si/Si SUBSTRATE USING RF-SPUTTERING AND E-BEAM EVAPORATOR TECHNIQUES.75

5.1 Optimization of GaN growth parameters using RF sputtering.....75

5.1.1 Effect of using different power and gas composition for GaN growth on Si substrate using RF-sputtering.....75

5.1.2 Preparation of nitride buffer layers using RF sputtering.....81

5.1.3 Growth of GaN layer on nitride buffer layer/Si substrate using RF sputtering.....85

5.1.4 Growth of GaN layer on porous Si/Si (100) substrates through RF sputtering.....94

5.2 Comparison of GaN layer grown on Si substrate, nitrides buffer layer/Si substrate and porous Si/Si substrate by RF sputtering.....98

5.2.1 Surface morphology of the GaN layers grown on different surfaces using Si substrates.....98

5.2.2 Structural properties of the GaN layers grown on different surfaces using Si substrate.....100

5.3 Optimization of GaN growth parameters using e-beam evaporator.....103

5.4 Comparison of GaN layer grown on Si substrate, RF sputtered nitrides buffer layer/Si substrate and porous Si/Si substrate using e-beam evaporator.....105

5.4.1 Surface morphology of the GaN layers grown on different surfaces using Si substrates.....106

5.4.2 Structural properties of the GaN layers grown on different surfaces using Si substrate.....109

5.5 Comparison of GaN layers grown by RF sputtering and e-beam evaporator.....111

5.6 Summary.....114

CHAPTER 6: EFFECT OF THERMAL ANNEALING TREATMENT ON GaN LAYER.....115

6.1 Optimizing thermal annealing conditions for GaN samples.....115

6.1.1 Effect of nitrogen (N₂) and ammonia (NH₃) gases in annealing treatment for GaN samples.....116

6.1.2 Effect of temperature in annealing treatment for GaN samples.....	119
6.1.3 Effect of flow rate in annealing treatment for GaN samples...	122
6.2 Properties of RF-sputtering grown GaN layer with post-annealing treatment in ammonia ambient.....	124
6.2.1 Investigation on the surface morphology of the annealed GaN layer grown on Si substrate, TiN buffer layer/Si substrate and porous Si/Si substrate by RF-sputtering.....	124
6.2.2 Investigation on the crystalline quality of the annealed GaN layer grown on Si substrate, TiN buffer layer/Si substrate and porous Si/Si substrate by RF-sputtering.....	128
6.2.3 Investigation on the optical properties of the annealed GaN layer grown on Si substrate, TiN buffer layer/Si substrate and porous Si/Si substrate by RF-sputtering.....	130
6.3 Properties of e-beam evaporator grown GaN layer with post-annealing treatment in ammonia ambient	134
6.3.1 Investigation on the surface morphology of the annealed GaN layer grown on Si substrate, TiN buffer layer/Si substrate and porous Si/Si substrate by e-beam evaporator	135
6.3.2 Investigation on the crystalline quality of the annealed GaN layer grown on Si substrate, TiN buffer layer/Si substrate and porous Si/Si substrate by e-beam evaporator	137
6.3.3 Investigation on the optical properties of the annealed GaN layer grown on TiN buffer layer/Si substrate and porous Si/Si substrate by e-beam evaporator	139
6.4 Comparative analysis on the annealed GaN on porous Si/Si substrate grown by RF sputtering and e-beam evaporator.....	144
6.5 Summary.....	148
CHAPTER 7: CONCLUSIONS AND FUTURE WORKS.....	149
REFERENCES.....	153
APPENDICES.....	163
Appendix 1.0.....	163
Appendix 2.0.....	164
Appendix 3.0.....	165
Appendix 4.0.....	166

Appendix 5.0.....	168
Appendix 6.0.....	170
Appendix 7.0.....	172
Appendix 8.0.....	174
Appendix 9.0.....	175
Appendix 10.0.....	176
Appendix 11.0.....	177
LIST OF PUBLICATIONS.....	178

LIST OF TABLES

	Page
Table 2.1: Basic properties of GaN structure at 300 K. The values were taken from [14].	8
Table 2.2: Summary of growth of GaN layer using different buffer layer on Si substrate.	15
Table 2.3: Influence of the etching parameters on the porosity of Si, as reported in several works.	18
Table 3.1: Details of etching parameters used in this work for producing optimum etching conditions.	29
Table 3.2: Details of the growth conditions for AlN and TiN buffer layer growth through RF sputtering.	32
Table 3.3: Summary of growth conditions for GaN layer through RF sputtering	34
Table 3.4: Summary of growth conditions for GaN layer through e-beam evaporator	37
Table 3.5: List of XRD orientations which corresponded to 2 theta position.	47
Table 3.6. List of main binding energy of GaN material with corresponded to its chemical bonding. The values were taken from [94].	53
Table 3.7. List of main GaN emissions for hexagonal GaN. The values are taken from [99].	55
Table 4.1. Details of porous Si/Si substrate with different ratio of HF and ethanol.	59
Table 4.2. Details of porous Si/Si substrate with the mixture of HF: C ₂ H ₅ OH (1:4) under different current density.	61
Table 4.3. Details of porous Si/Si substrate with different etching time in a mixture of HF: C ₂ H ₅ OH (1:4).	63
Table 4.4. Details of porous Si/Si substrate with different ratio of HF, ethanol and H ₂ O ₂	67
Table 4.5. Details of porous Si/Si substrate at different etching time in a mixture of HF: C ₂ H ₅ OH: H ₂ O ₂ (1:4:1).	69

Table 4.6. Details of porous Si/Si substrate with different ratio of HF and DMF.	71
Table 4.7. Details of porous Si/Si substrates with the different of etching time in mixture of HF and DMF (1:3).	73
Table 5.1. Details of GaN layers grown by RF-sputtering at different power and gas composition (in ratio).	76
Table 5.2. List of the AlN buffer layers, grown on Si substrate at different thickness at the power of 200 W with Ar:N ₂ gas ratio of 1:5 by RF sputtering	81
Table 5.3. List of TiN buffer layers, grown on Si substrate at different thickness at the power of 250 W with Ar:N ₂ gas ratio of 2:1 by RF sputtering.	81
Table 5.4. List of GaN samples grown on AlN and TiN materials on different thickness of buffer layers, with ~1.60 μm thick GaN grown by RF sputtering.	85
Table 5.5. Details of GaN samples grown on porous Si/Si substrates with different pore sizes by RF sputtering.	94
Table 5.6. Details of GaN layer grown on different surface of Si substrate by RF sputtering.	98
Table 5.7 Summary of GaN layer grown on different surfaces by e-beam evaporator.	106
Table 6.1: Details of the GaN samples, annealed in different gasses with corresponding annealing time.	116
Table 6.2: Details of the GaN samples grown by e-beam evaporator which were annealed at different NH ₃ flow rate with their corresponding time.	122
Table 6.3: Details of annealed GaN samples grown by RF sputtering with different type of surface.	124
Table 6.4. Details of annealed GaN samples grown by e-beam evaporator with different type of surface.	135
Table 6.5: Comparison between the properties of annealed GaN on porous Si/Si substrate grown by RF sputtering and e-beam evaporator.	147

LIST OF FIGURES

	Page
Figure 2.1: Atomic arrangement of hexagonal GaN structure in [0001] direction. The filled and empty circles represent the Ga and N atoms, respectively. The figures have been modified from [14].	7
Figure 2.2: Illustration of (a) polar and (b) non-polar GaN structure. (c) Top view of hexagonal GaN structure with non-polar direction. Images were taken and edited from [16].	9
Figure 2.3: Illustration of atomic arrangement between GaN on (a) Si (111) and (b) Si (100) substrate for lattice constant a in lattice structure. Images were taken and edited from [33].	12
Figure 2.4: Illustration of tensile stress mechanism between GaN and Si substrate. Image was taken and edited from [35].	13
Figure 2.5: Illustration of lattice arrangement in GaN layer with and without insertion of buffer layer. Figure source is modified from [36].	14
Figure 2.6: Illustration of atomic arrangement in GaN layer on porous Si substrate as the defects propagation in the GaN layer was minimized by the pores structure.	20
Figure 3.1: Summary of research methodology used in this project	25
Figure 3.2: Schematic diagram of electrochemical (EC) etching setup in this work.	29
Figure 3.3: A typical mechanism of sputtered atom in sputtering system. Image is taken and edited from [81].	31
Figure 3.4: Diagram of GaN structure grown on various surfaces using RF-sputtering that involved in this works.	33
Figure 3.5: Schematic diagram of e-beam evaporator at our laboratory. Image was edited from [82].	35
Figure 3.6: Diagram of GaN structure grown on variation of surface using e-beam evaporator that involved in this works.	36
Figure 3.7: 3-zones furnace system for annealing GaN layers grown by RF-sputtering and e-beam evaporator. The annealing was conducted at second zone.	39
Figure 3.8: Basic diagram of FESEM system. Image was taken and edited from [83].	41

Figure 3.9: Schematic diagram of AFM system (model AFM Dimension Edge® Bruker) taken from [85].	43
Figure 3.10: The aligned laser is monitored on photodiode (left) whereas the laser is brought close to the tips end (right).	44
Figure 3.11: The X-ray diffraction in a crystal structure taken from [86].	46
Figure 3.12: Mechanism of 2θ - ω scan performed in this work. In this measurement, the detector moved 2 times faster than movement of the sample (ω). Image taken from [86]	48
Figure 3.13: Reported XRD pattern of hexagonal GaN film on Si (100) substrate grown by molecular beam epitaxy (MBE), taken from [92].	49
Figure 3.14: Mechanism of ω -scan performed in this work. In this measurement, only sample is moving while the 2θ detector remains static. Image taken from [86]	50
Figure 3.15: The illustration of x-ray photoelectron spectroscopy measurement. Image was modified from [96].	52
Figure 3.16: Schematic diagram of photoluminescence and Raman system used in this work.	55
Figure 3.17: A reported Raman spectrum under scattering geometry of $z(x, \text{unpolarised}) \bar{z}$ on GaN film [98].	56
Figure 4.1: Morphology of porous Si/Si substrates under different ratio of HF and ethanol with (a) 2:1, (b) 1:3, and (c) 1:4, respectively at the magnification of 10 000x. Red circle shows the X-shaped pores appears at sample PS3.	60
Figure 4.2: Surface morphology of the porous Si samples with different current density of (a) 5 mA/cm ² , (b) 10 mA/cm ² , (c) 20 mA/cm ² , and (d) 25 mA/cm ² , measured by FESEM at magnification of 5 000 x.	62
Figure 4.3: FESEM images of porous Si morphology at (a) 5 min, (b) 10 min, (c) 20 min, (d) 30 min, (e) 40 min and (f) 60 min at the magnification of 5 000 x.	64
Figure 4.4: The graph of average pore size under different etching time.	65

Figure 4.5: Cross-sectional image of porous Si sidewalls under different etching time of a) 5 min, b) 10 min, c) 20 min, d) 30 min, e) 40 min and f) 60 min at the magnification of 5 000 x.	66
Figure 4.6: Dependence of average pores depth of porous Si on time of etching.	66
Figure 4.7: Surface morphology of porous Si/Si substrate etched at different electrolyte ratio of () 1:4:1 and (b) 1:4:2 between HF: C ₂ H ₅ OH: H ₂ O ₂ . The white circle in (b) shows the presence of Si membrane which covered some of the pores at magnification 10 000 x.	68
Figure 4.8: Morphology of the porous Si/Si substrate with the influenced of etching time of (a)10 minutes, (b) 20 minutes, (c) 30 minutes and (d) 40 minutes with chemical ratio HF: C ₂ H ₅ OH: H ₂ O ₂ (1:4:1) at the magnification of 1 000 x. Inset figure shows the image at higher magnification scale of 10 000 x.	70
Figure 4.9: Surface morphology of porous Si/Si substrate in the influenced of DMF ratio of; a) 1:3, b) 1:6 and c) 1:9, taken by FESEM at the magnification of 10 000 x. Inset figures shows the high magnification of FESEM on 40 000 x.	72
Figure 4.10: Surface morphology of porous Si/Si substrate at different etching time of (a) 5 minutes, (b) 10 minutes, (c) 20 minutes and (d) 30 minutes at the magnification of 20 000 x.	74
Figure 5.1: XRD pattern for (a) Sample BG1 and (b) Sample BG2, grown at the power of 50 W using RF-sputtering. Clearly, no evidence of GaN related peaks in the data.	76
Figure 5.2: XRD pattern for (a) Sample BG3, and (b) Sample BG4 grown at different gas composition using RF sputtering at 120 W. As shown in figure (b), the GaN peak appears at 33°.	78
Figure 5.3: XRD pattern for Sample BG5 grown at the gas ratio of Ar and N ₂ of 1:1 at 120 W by RF sputtering.	79
Figure 5.4: X-ray photoelectron spectra of (a) Ga 3d and (b) N 1s for GaN grown on Si substrate, (Sample BG5) grown by RF sputtering.	80
Figure 5.5: Surface morphology of nitrides buffer layers grown with different thickness through RF sputtering.	83
Figure 5.6: Estimated grain size of AlN and TiN buffer layers grown on Si substrate, respectively, as measured by FESEM.	84

Figure 5.7: 3D-AFM images of (a) AlN buffer layer and (b) TiN buffer layers with thickness of ~140 nm.	85
Figure 5.8: Surface morphology of GaN layer grown on AlN and TiN buffer layers under different thickness through RF sputtering growth at magnification of 100,000 x. The GaN layer grown on Si substrate (Sample G1) is also included for comparison.	87
Figure 5.9: Estimated average of RMS roughness for GaN layer grown on different thickness of the AlN and TiN buffer layers, respectively.	88
Figure 5.10: 3D-AFM images of GaN layers grown on (a) Si substrate, (b) 70 nm thick AlN buffer layer and (c) 70 nm thick TiN buffer layers.	89
Figure 5.11: XRD 2θ - ω scan data for GaN layer grown on a) AlN and b) TiN buffer layers through RF sputtering. XRD peak of GaN (10 $\bar{1}$ 0) can be observed at $\sim 33^\circ$ while Si- (100) substrate at $\sim 70^\circ$.	91
Figure 5.12: Estimated threading dislocations density of the GaN layer grown on different thickness of the buffer layers by RF sputtering. Inset figures showed the results of ω -scan for Sample G1, Sample GA2 and Sample GT3, respectively.	92
Figure 5.13: Estimated crystallite size of the GaN grown on different thickness of the buffer layers.	93
Figure 5.14: GaN overgrown layer on (a) 10 minutes, (b) 20 minutes and (c) 30 minutes-etched porous Si/Si substrates. Inset figure is the porous Si/Si substrate before the GaN growth.	95
Figure 5.15: Results of XRD peak of GaN layers grown on different etching time of porous Si/Si substrates using RF-sputtering.	96
Figure 5.16: (a) Results of XRD ω -scan of GaN layers grown on different etching time of porous Si/Si substrate using RF sputtering at peak $\sim 33^\circ$. (b) Peak width (FWHM) of the XRD ω -scan of GaN layers with their corresponding estimated threading dislocations density.	97
Figure 5.17: Surface morphology of GaN layer grown on (a) Si substrate, (b) AlN/Si substrate, (c) TiN/Si substrate and (d) porous Si/Si substrate by RF sputtering. Inset of figure (d) is the porous Si substrate before the GaN growth.	99
Figure 5.18: Surface roughness of GaN layer on (a) Si substrate, (b) AlN buffer layer, (c) TiN buffer layer and (d) porous Si/Si substrate, measured by AFM.	100

Figure 5.19: XRD of 2θ - ω scan for GaN layer on various surfaces of Si substrate by RF sputtering.	101
Figure 5.20 (a) XRD ω -scan for the GaN peak at $\sim 33^\circ$ and its corresponding FWHM of the GaN layers grown by RF sputtering. (b) Estimated FWHM and threading dislocations density in GaN layer with respect to the different surface using Si substrate.	103
Figure 5.21: XRD peak for the GaN sample grown on the Si substrates by e-beam evaporator. The GaN peak can be seen at $\sim 33^\circ$ and it is related to diffraction by $(10\bar{1}0)$ plane	105
Figure 5.22: Surface morphology of GaN grown on (a) Si substrate, (b) AlN buffer layer, (c) TiN buffer layer, and d) porous Si/Si substrate by e-beam evaporator. Red arrows showed the random direction of rod-like structure of GaN. Inset of figure (d) is the porous Si substrate before the GaN growth.	107
Figure 5.23: Cross-sectional image of Sample GE1 with the evidence of rod-like structures on the surface of the GaN layer and the variation of measured thickness of GaN.	107
Figure 5.24: Surface roughness of GaN layer on (a) Si substrate, (b) AlN buffer layer, (c) TiN buffer layer and (d) porous Si/Si substrate, measured by AFM.	108
Figure 5.25: XRD of 2θ - ω scan for GaN layer on (a) Si substrate, (b) AlN buffer layer, (c) TiN buffer layer, and (d) porous Si/Si substrate by e-beam evaporator	109
Figure 5.26: (a) XRD ω -scan for the GaN peak at $\sim 33^\circ$ and its corresponding FWHM of the GaN layers grown by e-beam evaporator. (b) Estimated FWHM and threading dislocations density in GaN layer with respect to the different surface using Si substrate.	111
Figure 5.27: Surface morphology of GaN grown on porous Si/Si substrate by (a) RF sputtering and (b) e-beam evaporator. Clearly, the formation of GaN nanocrystallite structure can be observed. Inset figure shows the corresponding side-view image of overgrown GaN on porous Si/Si substrate.	112
Figure 5.28: Comparison of estimated TDD between RF sputtering and e-beam evaporator grown GaN layer on different surfaces.	113
Figure 6.1: Dependence of FWHM of the XRD peak at $\sim 33^\circ$ on time of annealing in different ambient. Inset figure shows the 2θ - ω scan for the 30 minutes annealed GaN layer for in NH_3 ambient at temperature 650°C .	117
Figure 6.2: PL spectrum of Sample A2 grown by e-beam evaporator, after being annealed with NH_3 at 650°C . No luminescence signal of GaN can be observed.	119

Figure 6.3: Dependence of FWHM of XRD peak on temperature in NH ₃ ambient.	120
Figure 6.4: Comparison of PL spectra of annealed GaN sample at (a) 650°C and (b) 950°C.	121
Figure 6.5: Comparison of Raman spectra for annealed GaN sample at (a) 650°C and (b) 950°C	121
Figure 6.6: Dependence of FWHM of XRD peak with annealing time, with different of NH ₃ flow rate.	123
Figure 6.7: Surface morphology of GaN samples grown on different surfaces of the Si substrate by RF sputtering after being annealed with NH ₃ ambient at magnification of 50,000 x. Note that image of GR1 and GT2 have to be measured at 100,000 x for better image.	126
Figure 6.8: Surface roughness of GaN samples grown on (a) Si substrate, (b) TiN buffer layer/Si substrate and (c) porous Si/Si substrate after being annealed with NH ₃ ambient, as measured by AFM.	128
Figure 6.9: (a) XRD data of GaN layers grown on Si substrate, TiN buffer layer and porous Si/Si substrate, after being annealed with NH ₃ ambient. (b) The estimated TDD for the annealed GaN samples. Also included is the data of the non-annealed samples for easier comparison.	129
Figure 6.10: PL spectra of RF sputtering grown GaN samples, after being annealed with NH ₃ ambient. Inset figure shows the magnified NBE emission.	131
Figure 6.11: (a) Raman spectra of RF sputtering grown GaN samples, after being annealed with NH ₃ ambient. (b) FWHM of E ₂ (high) peak of annealed GaN samples grown by RF sputtering.	133
Figure 6.12: Surface morphology of GaN samples grown on different surface of the Si substrate by e-beam evaporator after being annealed with NH ₃ ambient at the magnification of 30,000 x.	136
Figure 6.13: Surface roughness of GaN samples grown on (a) Si substrate, (b) TiN buffer layer/Si substrate and (c) porous Si/Si substrate after being annealed with NH ₃ ambient, measured by AFM.	137
Figure 6.14: (a) XRD data of GaN layers grown on Si substrate, TiN buffer layer and porous Si/Si substrate, after being annealed with NH ₃ ambient. (b) The estimated TDD for the annealed GaN samples. Also included is the data of the non-annealed samples for easier comparison.	139

Figure 6.15: PL spectra of e-beam evaporator grown GaN samples, annealed in NH₃ ambient at 950°C for 30 minutes. Inset figure shows the FWHM of NBE emission of each samples. 141

Figure 6.16: (a) Raman scattering spectrum of GaN layers grown on Si substrate, TiN buffer layer/Si substrate and porous Si/Si substrate, after annealed with NH₃ ambient. (b) FWHM of the Raman peak at 568 cm⁻¹ of the annealed GaN. 143

Figure 6.17: Comparison between the morphology of the annealed GaN on porous Si/Si substrate grown by (a) RF sputtering and (b) e-beam evaporator at magnification of 30, 000x. Inset figure shows the corresponding side-view image of overgrown GaN on porous Si/Si substrate. 145

Figure 6.18: XRD data of annealed GaN on porous Si/Si substrate grown by different techniques. 146

Figure 6.19: Comparison of (a) PL and (b) Raman spectra between GaN sample grown by (i) RF-sputtering and (ii) e-beam evaporator. 147

LIST OF SYMBOLS

$^{\circ}$	Degree
$^{\circ}\text{C}$	Temperature in degree celcius
2θ	Diffraction angle in XRD (2 Theta)
a	Lattice constant in a -plane
\AA	Angstrom
b_a	Burger vector in a -plane
c	Lattice constant in c -plane
F^-	Flouride ion
K	Temperature in Kelvin
k	Scherrer Constant
ϕ	in-plane rocking curve
β	Integral width (FWHM)
λ	wavelength
ω	Diffraction angle in XRD (Omega)

LIST OF ABBREVIATIONS

AFM	Atomic Force Microscopy
Al	Aluminium
Al ₂ O ₃	Sapphire
AlN	Aluminium Nitride
Ar	Argon
C ₂ H ₅ OH	Ethanol acid
C ₃ H ₇ NO	Dimethylformamide
CL	Cathodoluminescence
CMOS	Complementary Metal Oxide Semiconductor
Cu	Copper
CVD	Chemical Vapour Deposition
DAP	Donor-acceptor pair
DC	Direct Current
DI	Deionized
DMF	Dimethylformamide
E-beam	Electron beam
EC	Electrochemical
ETD	Everhart-Thornley Detector
FEG	Field emission Gun
FESEM	Field Emission Scanning Electron Microscopy
FWHM	Full Width of Half Maximum
Ga	Gallium atom
GaAs	Gallium Arsenide
GaN	Gallium Nitride
H ₂	Hydrogen
H ₂ O	Water
H ₂ O ₂	Hydrogen Peroxide
HCL	Hydrochloric Acid
HeCd	Helium Cadmium
HEMTs	High-Electron Mobility Transistors
HF	Hydroflouric acid
HR-XRD	High Resolution X-ray Diffraction
LEDs	Light Emitting Diodes
LO	Longitudinal Optics
MBE	Molecular Beam Epitaxy
MFC	Mass Flow Controller
Min	Minute
MOCVD	Metal Organic Chemical Vapour Deposition
MOSFETs	Metal-Oxide-Semiconductor Field-Effect Transistors
N	Nitrogen atom

N ₂	Nitrogen
NBE	Near Band Edge
NH ₃	Ammonia
NH ₄ OH	Ammonium Hydroxide
OLEDs	Organic Light Emitting Diodes
PA	Phase Analysis (XRD)
PL	Photoluminescence
Pt	Platinum
PVD	Physical Vapour Deposition
RC	Rocking curve (XRD)
RCA	Radio Corporation of America
RF	Radio-Frequency
RMS	Root Mean Square
RSM	Reciprocal Space Mapping
SCCM	Standard Cubic Centimeters per Minute
Si	Silicon
SiC	Silicon Carbide
SLM	Standard Litres per Minute
SLS	Superlattices Structure
SSL	Solid State Lighting
TDD	Threading dislocations density
TEM	Transmission Electron Microscopy
TiN	Titanium Nitride
TLD	Through-the-Lens Detector
XPS	X-ray Photoelectron Spectroscopy
SIN _x	Silicon Nitride

PENUMBUHAN DAN PENCIRIAN LAPISAN GALLIUM NITRIDA KE ATAS SUBSTRAT SILIKON BERLIANG

ABSTRAK

Kajian ini memfokuskan penumbuhan lapisan gallium nitrida (GaN) ke atas substrat silikon (Si) berliang melalui kaedah percikan frekuensi radio (RF sputtering) dan penyejat alur elektron (e-beam evaporator). Untuk perbandingan, lapisan penampan nitrida aluminium nitrida (AlN), lapisan penampan titanium nitrida (TiN) dan substrat Si telah digunakan untuk penumbuhan lapisan GaN. Substrat Si berliang telah disediakan melalui kaedah punaran elektrokimia dengan menggunakan parameter yang berbeza. Didapati bahawa keliangan Si ini boleh dipengaruhi oleh jenis elektrolit (larutan), masa punaran dan ketumpatan arus. Hasil daripada pemerhatian, larutan dimethylformamide (DMF) dengan tempoh punaran 30 minit pada 10 mA/cm^2 ketumpatan arus dapat menghasilkan struktur keliangan Si yang paling optimum. Seterusnya, lapisan GaN telah ditumbuhkan pada Si berliang, lapisan penampan nitrida dan substrat Si melalui percikan frekuensi radio dan penyejat alur elektron. Seperti mana yang telah diukur daripada pengukuran mikroskop elektron pengimbas pancaran medan (FESEM) dan mikroskop daya atom (AFM), lapisan penampan nitrida menghasilkan permukaan GaN yang halus manakala Si berliang menghasilkan permukaan GaN yang kasar, terutamanya pada penumbuhan GaN melalui penyejat alur elektron. Pengukuran pembelauan sinar-X (XRD) menunjukkan bahawa semua sampel GaN yang tidak disepuh-lindap lebih sesuai ditumbuhi dalam GaN bukan terkutub (non-polar) berorientasi ($10\bar{1}0$). Imbasan- ω XRD menunjukkan bahawa lebar lengkap separa maksimum (FWHM) untuk puncak GaN pada lapisan GaN diatas substrat Si berliang adalah yang paling kecil berbanding dengan sampel-sampel yang lain, dengan penghasilan ketumpatan perkehelan berulir sebanyak $\sim 10^8 \text{ cm}^{-2}$, terutamanya untuk penumbuhan lapisan GaN melalui kaedah percikan RF. Walau

bagaimanapun, semua lapisan GaN yang tidak disepuh-lindap menghasilkan kualiti optik yang tidak memberangsangkan oleh kerana tiada puncak yang berkaitan dengan bahan GaN dapat dikesan pada spektrum fotoluminesens dan Raman. Untuk mengurangkan masalah ini, rawatan pasca-penyepuhlindapan dalam persekitaran ammonia (NH_3) pada suhu 950°C selama 30 minit telah dicadangkan. Pengukuran FESEM menunjukkan bahawa semua lapisan GaN yang telah disepuh-lindap mempamerkan permukaan kasar dan berfaset-heksagon. Selain itu, semua lapisan GaN yang disepuh-lindap juga didapati lebih sesuai ditumbuhi dalam struktur polihabluran dengan puncak-puncak yang signifikan pada satah $(10\bar{1}0)$, (0002) , and $(10\bar{1}1)$, seperti yang disahkan melalui imbasan 2θ - ω XRD. Imbasan- ω XRD menunjukkan bahawa ketumpatan perkehelen berulir semakin berkurang berbanding dengan sampel-sampel yang tidak disepuh-lindap, terutamanya untuk lapisan GaN pada Si berliang melalui kaedah penyejat alur elektron. Walaupun permukaan lapisan sedikit kasar, namun sifat-sifat optikal untuk lapisan-lapisan GaN ini didapati lebih baik dengan pancaran pinggir jalur dekat (NBE) dan GaN E_2 (high) yang signifikan berbanding dengan sampel-sampel yang tidak disepuh-lindap.

GROWTH AND CHARACTERIZATION OF GALLIUM NITRIDE FILMS ON POROUS SILICON SUBSTRATE

ABSTRACT

This work focuses on the growth of GaN films on porous Si/Si substrate by radio frequency (RF) sputtering and electron beam (e-beam) evaporator. As a comparison, aluminium nitride (AlN) buffer layer, titanium nitride (TiN) buffer layer and Si substrate were used to grow the GaN layer. Porous Si/Si substrate was initially prepared by electrochemical etching using different parameters. It was found that the porosity of Si could be influenced by the type of electrolyte (solution), etching time and current density. From the observations, the dimethylformamide (DMF) solution with 30 minutes etched, under 10 mA/cm^2 of current density produced the optimum porous structure. Next, the GaN layers were grown on Si substrate, nitrides buffer layers/Si substrate and porous Si/Si substrate by RF sputtering and e-beam evaporator, respectively. As witnessed from field emission scanning electron microscopy (FESEM) and atomic force microscopy (AFM) measurements, the nitrides buffer layers gave smoother GaN surface while the porous Si resulted in rougher GaN surface, particularly for e-beam evaporator growth GaN layer. X-ray diffraction (XRD) measurements revealed that all non-annealed GaN samples were preferably grown in non-polar GaN of $(10\bar{1}0)$ orientation. The XRD ω -scan revealed that the FWHM of the GaN peak was found to be narrow in the GaN layer on porous Si/Si substrate among others, implying the lowest threading dislocations density in the sample at $\sim 10^8 \text{ cm}^{-2}$, especially for RF sputtering growth GaN layer. However, the optical quality for all non-annealed GaN layers appeared to be poor since no peak related to GaN material can be detected in photoluminescence (PL) and Raman spectra. To address this problem, post-annealing treatment in ammonia (NH_3) ambient

at 950°C for 30 minutes was proposed. FESEM measurement revealed that all the annealed GaN layers turned into rough and distinguished hexagonal-faceted grains. In addition, the annealed GaN layers were found to be grown in polycrystalline structure with significant peaks at $(10\bar{1}0)$, (0002) , and $(10\bar{1}1)$ planes, as confirmed by XRD 2θ - ω scan. The XRD ω -scan revealed that the threading dislocations density showed further reduction as compared to the non-annealed samples, especially for GaN on porous Si sample grown by e-beam evaporator. It is worth to note, despite of a rough surface, the optical properties of the annealed GaN layers greatly improved with significant near band edge (NBE) emission and GaN E_2 (high) as compared to non-annealed samples.

CHAPTER 1

INTRODUCTION TO GaN SEMICONDUCTOR

Gallium nitride (GaN) material has received great attentions and attractions since few decades ago. This is due to its high breakdown voltage, large critical electric field and high thermal conductivity. Such properties are beneficial for electronic devices such as metal-oxide-semiconductor field-effect transistors (MOSFETs), high-electron mobility transistors (HEMTs), and Schottky diodes to operate at higher voltage levels, help in reducing switching losses and offer better power efficiency than other semiconductor materials [1]. In the latest advancement of the GaN technology, most of the GaN based power devices application involved in radio-frequency (RF) devices, inverters/converters, motor drivers and power supply are being used extensively [1].

In the aspects of optoelectronics devices like light emitting diodes (LEDs) and laser diode, the GaN material has wide and direct band gap, which allows the devices base on it to emit at shorter wavelength (365 nm). At this wavelength, the optical properties of the GaN devices exhibit ultra-high brightness emission, which gives significant rewards to solid-state lighting (SSL¹) application, especially in LEDs. According to annual report of Department of Energy, United State 2014, SSL technology is expected to promote light saving energy up to one-third of the electricity consumption, twelve times higher than solar cell by 2025 [2].

¹ SSL refers to the family of solid state lighting technologies with high potential to replace the conventional light, fluorescence and incandescent lamps. Examples of SSL devices are light emitting diodes (LEDs), laser diodes and organic light emitting diodes (OLEDs) that have been used in display board, traffic light and in camera flash.

Problem statement and motivation of study

Notwithstanding all the advantages of GaN based devices and materials, there are persistence unsolved problem related to the quality of this material and the stability of the GaN devices. Homoepitaxial growth of GaN devices on GaN substrate is very limited due to the difficulty to produce a high quality of bulk GaN and expensive. The use of foreign substrate like sapphire (Al_2O_3), gallium arsenide (GaAs), silicon carbide (SiC) and silicon (Si) become an alternative substrates to grow GaN based devices. Among them, Si becomes the most potential substrate, especially in mass-production level due to its inexpensive price and availability in larger size. However, the issue in the growth of the GaN layer on Si substrate is mainly related to the lattice mismatch and thermal expansion between the epitaxial layer and the substrate. As a result, the GaN layer typically contains high defects density and cracks in the GaN layer [3].

The introduction of a buffer layer between the GaN layer and the Si substrate is a common strategy to ameliorate such problems. Nonetheless, the threading dislocation² remains high, which can limit the efficiency of the GaN based devices and reduce their phonon lifetime. In this work, the use of porous Si layer on the Si substrate could be a better solution to further reduce the impact from the lattice mismatch [4-5]. The void spaces of the porous Si surface could significantly ‘sink-out’ the threading dislocation while release strain in the GaN layer.

Recently, numerous techniques have been developed to grow GaN on Si substrate. The growth of GaN layers through physical vapour deposition (PVD), e.g molecular beam epitaxy (MBE) [6, 7], radio frequency (RF) sputtering [8, 9] and

² Categorize as one type of line defect. It happens when there is a large difference in atomic arrangement between epitaxial layer and substrate. Threading dislocations defect in semiconductor can create electrical charge trapping and reduced the number of available carriers.

electron beam (e-beam) evaporator [10] can be considered as among the most convenient method for thin film growth. This is because the GaN layer can be grown at lower risk³ than chemical vapour deposition (CVD). However, RF sputtering and e-beam evaporator are more preferable technique to grow GaN layer since both techniques are simple and inexpensive technique than MBE.

It is well-known that the GaN films typically contains strong spontaneous and piezoelectric polarizations when it is grown along the [0001] direction. This subsequently leads to the degradation of overlapping of electron and hole wave function, which limits the performance of optoelectronic devices [11]. To eliminate such behaviour, the growth of GaN layers in non-polar orientation, e.g (10 $\bar{1}$ 0) or (11 $\bar{2}$ 0), is desirable. If a non-polar GaN layer can be grown using simple and inexpensive technique like RF sputtering and e-beam evaporator, it would open more explorations that would lead to significant development in GaN technology.

Scope of study and objectives of the research

This study focuses on the growth GaN on porous Si/Si substrate for good quality of GaN layer. The aim of this project is to study the effectiveness of using porous Si as a surface to grow GaN on it. Therefore, the main objectives of this thesis are;

- 1) to fabricate porous Si using electrochemical etching with a good uniformity and porosity of the pores.

³ Physical vapour deposition (PVD) appeared to be safer than chemical vapour deposition (CVD) since it involved with the absent of dangerous gas such as trimethylGallium (TMGa), trimethylAluminium and silane, which can explode if exposed to air. Most of the PVD process used nitrogen (N₂) plasma as a source for nitride material.

- 2) to grow GaN layer on porous Si substrate using radio-frequency (RF) sputtering and electron beam (e-beam) evaporator and investigating the surface morphology, structural and optical properties of the GaN samples.
- 3) to improve the properties of the GaN on porous Si layer using post-annealing treatment under ammonia (NH₃).

In addition to that, GaN layer was also grown on Si substrate, aluminium nitride (AlN) and titanium nitride (TiN) buffer layers for comparison.

The contents of this thesis have been organized as follows:

Chapter 2 encompasses the structural properties and the basic properties of GaN materials. Progress works on GaN growth on Si substrate, fabrication of porous Si substrates, and annealing background are reviewed.

Chapter 3, the readers will be exposed to the experimental procedures that describes the etching process, the growth process of GaN, annealing process and characterization measurement, which had been performed in this project. Problems and issues that have encountered during the experiments will be discussed and the solutions are suggested to improve the outputs and data collections.

Chapter 4 will be focusing on the fabrication of the porous Si (100)-oriented substrates using electrochemical etching in different etching conditions. The results are presented, particularly on surface morphology, as measured by field emission scanning electron microscopy (FESEM). The optimum etching parameters that produce high porosity and uniformity of porous Si will be proposed as a surface for the subsequent GaN layer.

Chapter 5 presents the properties of the GaN layer grown directly on the porous Si substrate, including with the nitrides buffer layer (AlN and TiN) and Si substrate using RF sputtering and e-beam evaporator. The optimization of the GaN growth conditions will be discussed. The results of GaN samples grown on porous Si/Si substrate and the nitrides buffer layer/Si substrate will be presented based on the morphology, structural and optical properties of the samples.

Chapter 6 reports the effect of post-annealing treatment on the grown GaN sample by RF sputtering and e-beam evaporator, with different conditions. The analysis will cover the surface morphology, crystalline quality and optical quality of the annealed GaN samples. The comparison between RF sputtering and e-beam evaporator will be provided in order to propose the best GaN growth.

Chapter 7 is the final chapter that concludes the findings of the research works. This will be ended by several suggestions for the future works to improve the quality of this research project.

CHAPTER 2

BASIC PROPERTIES AND LITERATURE REVIEW OF GaN

This chapter begins with a discussion of the fundamental properties of GaN material so that the understanding on the material can be well-established. Subsequently, a detailed review on growing GaN on Si substrate, including the use of buffer layer will be given. It has been reported that the porous Si/Si substrate is a new technique to allow better growth of GaN directly onto Si substrate. With this regards, the introduction of porous Si and its fabrication will be presented here. This is followed by a review on the growth of GaN onto porous Si/Si substrate across literature. Apart from that, technique of growing GaN using inexpensive and simple manner will be discussed. This chapter ends with a survey on improving the crystalline quality of GaN material through annealing treatment.

2.1 Introduction to GaN material.

Gallium nitride (GaN) material is considered as one of the most important materials in advanced devices. This material possesses a wide and direct band gap of 3.4 eV that allow devices based on them such as light emitting diodes (LEDs), laser and transistors (high-electron-mobility transistors, HEMTs) to operate at high temperature, frequency and power [12, 13]. Recently, Professor Shuji Nakamura has won the Nobel Prize in Physics in 2014 upon his significant contribution in developing blue LEDs based on GaN towards white light production.

2.1.1 Basic crystal structure of GaN material.

GaN can generally exist in two phases; 1) hexagonal (wurtzite) and 2) cubic (zinc-blende) [14]. Hexagonal GaN is a thermodynamically stable structure, whereas

cubic GaN is a metastable structure. Therefore, specific growth conditions are required to grow GaN with different phase material. Details of the illustration of the atomic arrangement in hexagonal GaN structure are shown as in Figure 2.1. In general, the hexagonal GaN structure consists of two lattice constants, which a refers to the distance between two atoms at the basal plane while c associates to the distance perpendicular to the basal plane. Each Ga atom is bonded to four neighbouring nitrogen atoms. Similarly, each nitrogen atom is bonded to four Ga atoms (see figure 2.1). The stacking sequence of the GaN hexagonal-closed packed in the $\langle 0001 \rangle$ plane is ABABAB along the $[0001]$ axis, where the capital letter A is denoted as a distinctive of Ga cation (Ga^{3+}) whilst the capital letter B is denoted as nitrogen anion (N^{3-}) position in the triangular lattice on the (0001) .

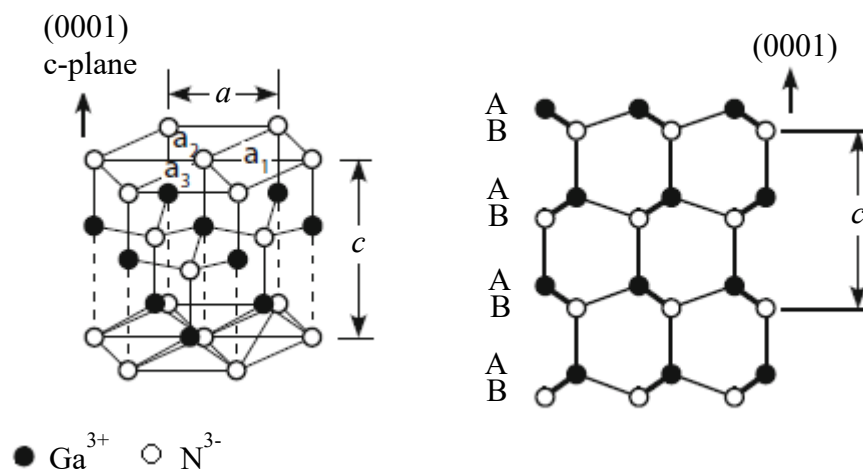


Figure 2.1: Atomic arrangement of hexagonal GaN structure in $[0001]$ direction. The filled and empty circles represent the Ga and N atoms, respectively. The figures have been modified from [14].

Table 2.1 shows the basic properties of the hexagonal GaN structure, at 300 K and these values are commonly used in many works [14, 15]. However, these values are dependent and affected by the variation of built-in strain from different growth. Theoretically, the arrangement of lattice constants are strongly depending on the

strain-induced defects inside the materials. This will highly affect the crystalline and optical quality of the GaN layer.

Table 2.1: Basic properties of GaN structure at 300 K. The values were taken from [14].

Structure	Wurtzite
Symmetry	Hexagonal
Stability	Stable
Energy Gap (eV)	3.400
Lattice constant, a (Å)	3.189
Lattice constant, b (Å)	5.185
E_2 (high) phonon mode (cm^{-1})	568
A_1 (LO) phonon mode (cm^{-1})	734

Apart from polar direction, GaN also can be grown in $(10\bar{1}0)$ orientation. This kind of plane orientation is non-polar, of which free from piezoelectric and spontaneous effects. So far, works on developing GaN in non-polar $(10\bar{1}0)$ plane are increasingly conducted to realize super powerful devices in future. Figure 2.2 shows the illustrated structure of non-polar plane in comparison with polar plane. Unlike $(10\bar{1}0)$ orientation, which occurs on m-plane, non-polar a-plane in $(11\bar{2}0)$ is hardly to be achieved without proper growth preparations.

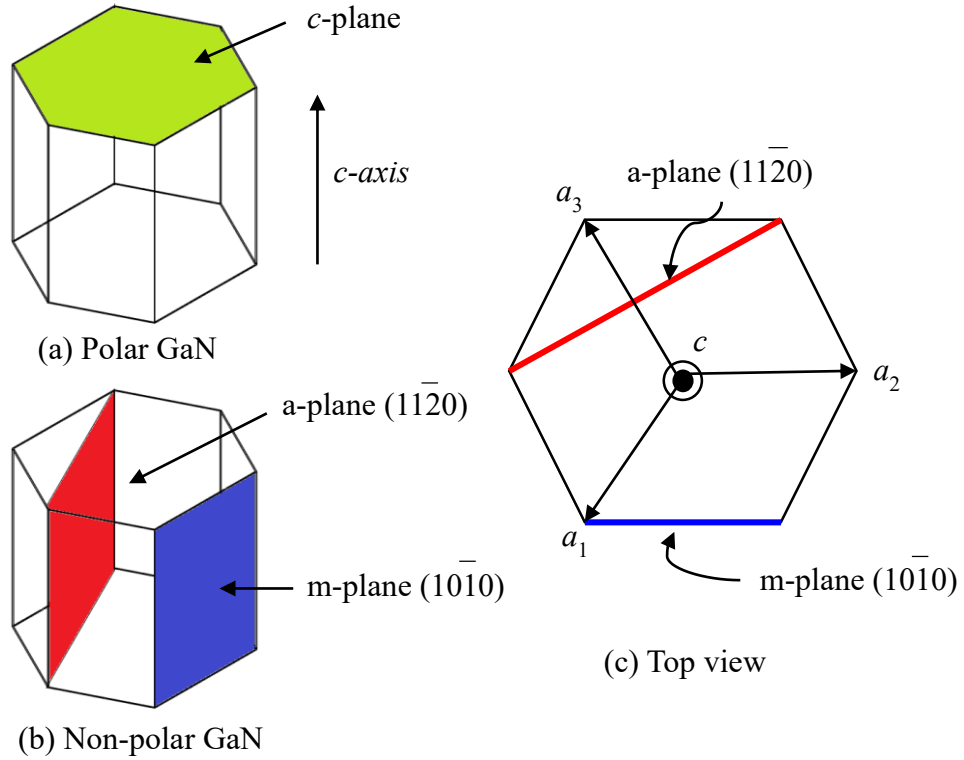


Figure 2.2: Illustration of (a) polar and (b) non-polar GaN structure. (c) Top view of hexagonal GaN structure with non-polar direction. Images were taken and edited from [16].

2.2 Growing GaN on Si substrate and its general issues.

Homoepitaxial growth of GaN devices on GaN substrate is very limited due to the difficulty to produce a high quality bulk GaN. Alternatively, foreign substrates like sapphire (Al_2O_3), gallium arsenide (GaAs), silicon carbide (SiC) and silicon (Si) substrates have a potential to grow the heteroepitaxial GaN. The following section will clarify the progress in growing GaN for heteroepitaxy growth.

2.2.1. Progress of GaN growth onto Si substrate.

Recently, Al_2O_3 , GaAs and SiC materials are the most popular substrates for heteroepitaxial GaN growth. Nonetheless, these substrates are rather costly, limited in size and impossible to be produced in large scale [17]. Therefore, silicon (Si) becomes the most preferable substrate for GaN epitaxy since it is available in a large size, good

in thermal conductivity, easy cleaving along the substrate facet, low cost, and also exhibits good uniformity of carrier injection which is beneficial for nitride based devices and structures [18-20]. Hence, this section will clarify the use of Si substrate for GaN growth and issues pertaining to the GaN growth onto the Si substrate.

From the history point of view, Roessner and his team members [21] had showed the interest of growing a GaN on Si substrate in the year of 1995. They demonstrated the epitaxial growth of GaN on top of the Si substrate using electron cyclotron resonance plasma-assisted molecular beam epitaxy (MBE). Under different cleaning preparation of Si wafer via Shiraki method and Radio Corporation of America (RCA) method, this team managed to obtain polycrystalline structure of hexagonal GaN film on Si (001) substrate. However, the potential of their GaN is constrained due to high defect density. A few years later, Guha and Bojarczuk discovered the first MBE growth of GaN based LEDs on Si substrate [22] by initiating the use of the bottom contact for electron injection to the device structure through a thin AlN growth initiation layer. They also demonstrated the *p*-type doping that is achievable in GaN on Si substrate. This is a starting point to show the ability of growing GaN based devices using Si substrate.

In 2002, Krost et.al. [23] demonstrated the growth of GaN-based optoelectronics on Si substrate with cost-effective LEDs via metal organic chemical vapour deposition (MOCVD). They succeeded to achieve a high optical output power of GaN based Si LEDs with 100 μ W at forward voltage of 20 mA. This value is far greater than the output power of LEDs based GaN on Al₂O₃ (42 μ W) and SiC (70 μ W), as demonstrated by Nakamura et.al [24] and Gosei et.al. [25], respectively. Through this comparison, the integration of optoelectronics devices based on GaN on Si substrate exhibits better performance than the GaN devices on Al₂O₃ and SiC. So

far, GaN layers were mainly grown in [0001] orientation using Si substrate. It is very hard to achieve (10 $\bar{1}$ 0) GaN structure without significant adjustment required in the growth conditions.

2.2.2 Si substrate orientation: Si (111) versus Si (100).

In most reports, the hexagonal GaN layers were grown onto Si (111)-oriented substrates using MBE [6,7] and MOCVD [26,27]. The reason of using Si (111) orientation is mainly due to the three-folded symmetry⁴ of this plane, served as a template for hexagonal GaN crystal structure. Nonetheless, there are some problems related to the integration of the GaN on Si (111) based devices, for example the GaN-on-Si (111) LEDs. A group from Taiwan, Shen et. al. [28] reported that it is hard to etch Si (111) substrate due to its large energy bonding, thus resulting in an extended time period of etching process that is subsequently damaging to the crystalline properties of the GaN-on-Si (111) LEDs.

Unlike Si (111) substrate, the Si (100)-oriented substrate offers an easy substrates removal with 20 times faster than the etching rate in Si (111)-oriented substrate due to a small bonding energy of Si atoms [28]. This gives extra advantages to Si (100)-oriented substrate for integration of high performance of GaN-on-Si (100) based devices such as in LEDs, complementary metal oxide semiconductor (CMOS) and high electron mobility transistor (HEMT) [29-31]. Furthermore, the substrates cleaving of Si (100)-oriented is easier without damaging the wafer as compared to the Si (111)-oriented substrate. Besides, Si (100) is preferable as the substrate for GaN as it has much fewer interface defect than Si (111) due to much smaller lattice constant

⁴ Object that repeat itself upon rotation of 120°. The three fold symmetry will match at 120°, 240° and 360°.

thus making GaN layer with less defect density is possible [32]. Figure 2.3 shows the illustration of lattice constant for GaN on Si (111) and Si (100), respectively

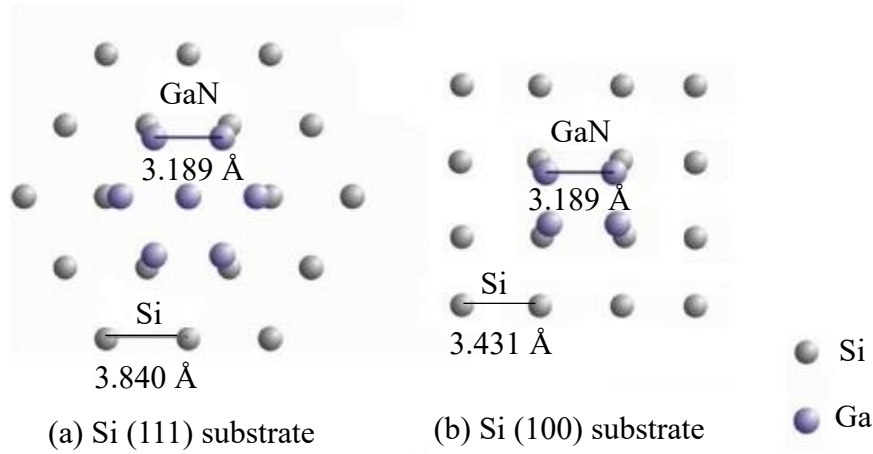


Figure 2.3: Illustration of atomic arrangement between GaN on (a) Si (111) and (b) Si (100) substrate for lattice constant a in lattice structure. Images were taken and edited from [33].

2.2.3 Issue on growing GaN on Si substrate.

Direct growth of GaN on Si (100) substrate is quite challenging as the layer commonly suffers from high threading dislocations density and cracks that lead to degradation of optical and electrical properties of devices. Theoretically, the atomic arrangement between both materials is far from ideal in term of lattice mismatch and thermal expansion coefficient. The lattice mismatch between GaN and Si is reported to be around 17%, due to a large difference between lattice constant of both materials [17]. Furthermore, the thermal expansion of GaN is two times lower than the Si substrate ($\sim 54\%$), which subsequently contributed to the formation of cracks on the GaN surface upon cooling phase [34]. As a result, the growth of a thick GaN layer (above critical thickness ~ 300 nm) on Si substrate is very unlikely without cracks.

In general, direct growth of GaN on Si will exhibit tensile stress in order to conform the lattice structure of the substrate. This is mainly due to the large lattice constant a of Si substrate (3.431\AA) with respect to the lattice constant a of GaN (3.189\AA). Figure 2.4 shows the common mechanism of tensile stress mechanism in epitaxy. Such condition will lead to the formation of cracks and induce propagation of defects; e.g. threading dislocations toward the GaN surface and limits the potential of GaN applications. In order to minimize these problems, some alternative efforts have been proposed as to reduce the impact from the large difference in atomic arrangement between GaN and Si. The following section describes the improvement of GaN overgrown layer using several techniques.

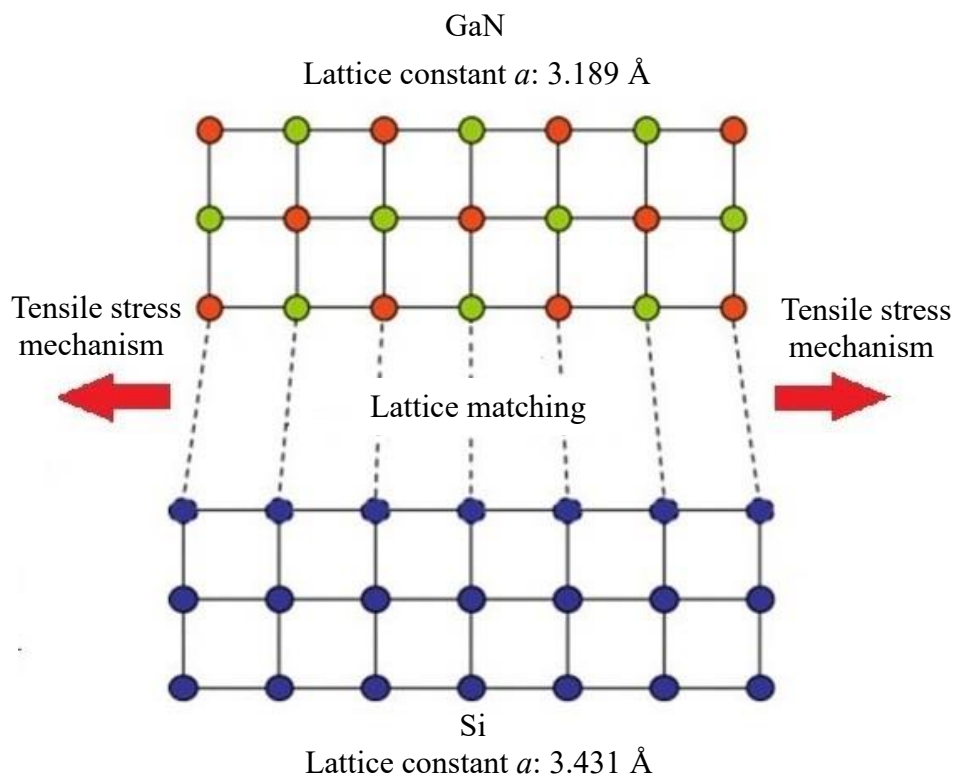


Figure 2.4: Illustration of tensile stress mechanism between GaN and Si substrate. Image was taken and edited from [35].

2.3 Role of buffer layer in GaN growth on Si substrate.

A buffer layer is typically grown directly on the substrate prior to the GaN growth. As a matter of fact, introduction of buffer layer into the growth of GaN heterostructure is a common way to compensate the tensile stress and preclude the crack formation. Figure 2.5 shows the lattice arrangement of GaN layer on Si substrate, with and without buffer layer. This illustration shows that with the presence of buffer layer, the GaN overgrown layer exhibits a better structure.

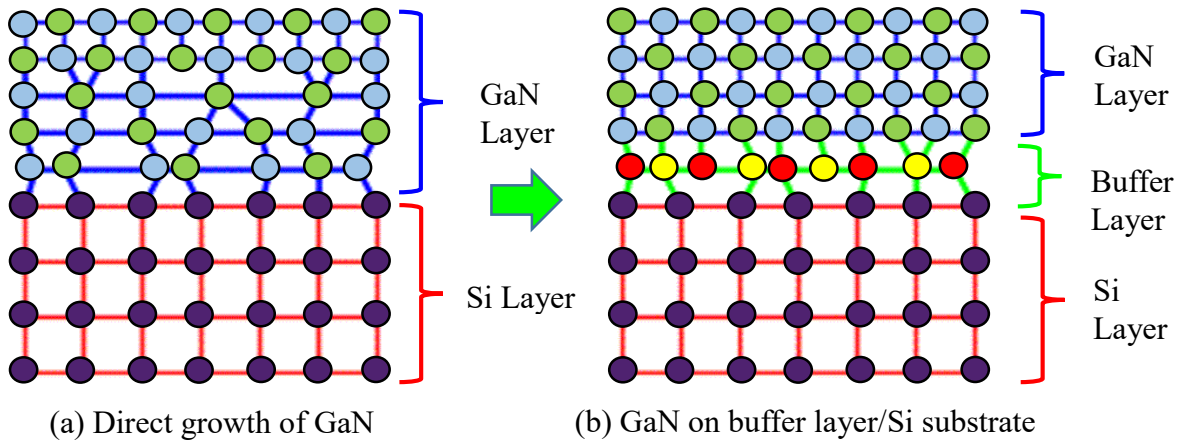


Figure 2.5: Illustration of lattice arrangement in GaN layer with and without insertion of buffer layer. Figure source is modified from [36].

Up to date, numerous buffer layers have been employed such as SiC [7, 37-38], aluminium nitride (AlN) [39, 40] and titanium nitride (TiN) [41, 42]. Apart from that, AlN/GaN superlattices stack layer [43, 44] has been used to improve GaN growth. Review on the published research on the use of various buffer layers for GaN on Si growth are summarized in Table 2.2. In general, SiC buffer layer is one of the candidates for growing GaN layer onto the Si substrate. For example, As et.al [7] and Wang et.al [37] are among the pioneer in developing better quality GaN on Si growth using a flat SiC buffer layer through the MBE. They revealed that SiC is very useful

in suppressing the formation of amorphous silicon nitride (SiN_x) and therefore can promote into better optical quality. However, the growth of SiC buffer layer onto the Si substrate naturally exhibits rough SiC/Si interface, which contains high impurities and gives poor single crystal quality that would affect the properties of the GaN overgrown layer [38].

Table 2.2: Summary of growth of GaN layer using different buffer layers on Si substrate.

Buffer layer	Advantage	Disadvantage	Reference
SiC	-Promotes better optical properties -Good suppression for SiN_x formation	-Exhibit rough surface -High level background impurities	[7,36-38]
AlN	-Small lattice mismatch (2.5%) -Good wettability to GaN	-Insulative behaviour -Optimized thickness is extremely critical	[39, 40]
TiN	-Small lattice mismatch (6.2%) - Conductive behaviour	- Never been applied on Si substrate	[41, 42]
AlN/GaN SLS	-Effectively reduce crack formation	-Very complex -Difficult to maintain uniformity of each layer	[43, 44]

AlN material is a common buffer layer for GaN epitaxy due to its ability to enhance the GaN nucleation, which in turn produces a layer with a mirror-like surface. In term of the lattice arrangement of the AlN material, it has a small number of lattice mismatch (2.5%) and thermal expansion coefficient (34.6%) with respect to the GaN as compared to GaN on the Si materials [39]. However, the thickness of the buffer layer should be optimized in order to achieve the crack-free GaN layer. For example, Yang et.al [40] investigated the effect of different thickness of AlN buffer layer for

the GaN growth on the Si substrate by using MOCVD. They found that the grown thin layer (<20 nm) and thick layer (>100 nm) of AlN had low crystallinity, which affected the coalescence behaviour of the GaN grains. Nonetheless, the AlN buffer layer with the thickness of 50 nm improved the GaN layer. Despite of this, AlN buffer layer tends to promote high charging effect⁵ because it is naturally an insulator material. This is not preferable for vertical transport devices.

On the other hand, titanium nitride (TiN) has the potential to be a good buffer layer to GaN since it exhibits smaller lattice mismatch of 6.2% [41]. The advantages of TiN lies on its better electrically conducting and its ability to promote the continuous growth, which results in a flat surface of GaN. This has been demonstrated by Watanabe et.al [41]. They successfully grew a good GaN layer with smooth and flat surface using TiN buffer layer. Like AlN buffer layer, the thickness of the TiN buffer layer plays a role in improving the GaN overgrown layer. The effect of using different thickness of the TiN buffer layer on GaN properties was reported by Ito et.al [42]. They revealed that GaN growth was better with the use of the TiN buffer layer at the thickness of 2 to 5 nm. Nonetheless, the above reports only focused on growing GaN layer using TiN buffer layer on sapphire substrate. To the best of our knowledge, TiN buffer layer has never been used in the growth of GaN on Si substrate.

The growth of the GaN can be improved using superlattices structure (SLS). This has been demonstrated by Eric et.al. [43] with the use of AlN/GaN SLS to prevent propagation of threading dislocation into the GaN layer to minimize cracks. The crystalline quality of the GaN layer is significantly enhanced by optimizing the number of SLS layer. Similar finding was also observed in [44], using AlN/GaN SLS.

⁵ See page 42

Nevertheless, the growth of SLS is challenging due to its complexity to maintain uniformed layer of the structure, especially in a very thin layer about few nanometers.

In this study, the introduction of the buffer layer is a classic way to grow GaN with minimum defects and strains. The structural and optical properties of the GaN layers with the presence of the buffer layer were reported to be improved. However the dislocations density remains high, around 10^9 - 10^{11} cm^{-2} [39,42]. In recent year, porous Si has received much attentions as the structure could ‘sink-out’ the strains and dislocations tremendously from propagating into the subsequent layer. This gives a new hope to growth scientists to grow GaN layer directly onto the Si substrate without concerning much on the problems resulted from the large lattice mismatch. Review of published works on the production of porous Si on Si substrate will be discussed as follow.

2.4 Introduction of porous Si and its fabrication.

Porous Si structure particularly offers high surface area to volume ratio that would lead to better external efficiency⁶ of devices like LEDs. The main ability of the porous Si lies on its void spaces feature that minimize defects and strains from propagating into the overgrown layer. There are several techniques used to develop porous Si e.g. laser-induced etching [45,46], electroless etching [47,48] and electrochemical etching [49-52]. Among these, the electrochemical (EC) etching is the most favourable technique due to its low surface damage, low cost and easy to operate. More interesting point about this method is that the uniformity of the porous Si is controllable by adjusting the related parameters. Currently, a number of works on EC etching has been demonstrated on porous Si [49-52]. The fabrication of porous is

⁶ Strong light extraction which reflected from porous sidewalls.

generally depending on parameters which are; 1) chemical solution based acid (hydrofluoric), 2) time of etching and 3) current density. Table 2.3 highlights the role of these parameters on controlling the porosity of Si.

Table 2.3: Influence of the etching parameters on the porosity of Si, as reported in several works.

Etching parameter	Research finding	Reference
Chemical solution	The pores structure depends on the type of the chemical used	[49, 53-54]
Etching time	Shorter time leads to small pores while longer period of time gives larger pores	[55-57]
Current density	Tend to destroy the pore structure if current is too high	[58-59]

Generally, numerous chemical solutions have been developed in order to prepare the porous structure using EC etching. For example, ethanol (C_2H_5OH) is widely used as a chemical solution to fabricate the porous Si layer due to its ability to initiate pores formation. Nevertheless, ethanol tends to promote high surface tension to the Si surface, which then leads to the formation of irregular pores, as reported in [49-52]. However, such problem can be eliminated by diversifying the type of the chemical solution. The use of hydrogen peroxide (H_2O_2) and dimethylformamide (DMF) can exterminate the wetting⁷ problem to the Si surface and consequently results in better Si porosity. For example, Splinter et.al. [53] introduced H_2O_2 in the mixture of HF and C_2H_5OH . Good uniformity and well-defined pores were formed at the ratio of 1:4:1 for HF: H_2O_2 : C_2H_5OH , respectively. On the other hand, direct mixing of DMF in HF solution results in high pores distribution. As compared to H_2O_2 , the Si

⁷ Ability of liquid to form interface with substrate surface. In such case, wetting defect can occur, e.g. poor adhesion of chemical solution.

porosity is further improved due to low surface tension and reductions of oxides formation [60-61].

Note that, time of etching and applied current density, both play major roles to form porous Si. Investigation on various etching time for porous Si were reported by Jeyakumaran et.al [55] at various time from 10 to 40 minutes. They revealed that the pores size was bigger as the etching time increased. Similar behaviour also has been observed in Milani et.al [56] and Lu et.al [57]. Longer time of etching will cause several pores to coalesce with their neighbouring pores and this results in larger pores. From both reports, the optimum etching time was found to be around 20 to 30 minutes.

On the contrary, the pores structure tends to diminish if the current density were set too high. Some reports had claimed that the optimum value of current density for n-type porous Si was 10 mA/cm² [58, 59]. The applied current density in each experiment must be kept constant during etching process in order to accommodate uniform pores distributions. Zhang et.al [51] proposed that the porosity of Si is uniform with the use of a constant current density. Similar to the case of optimizing the etching time, the pore size was found to be larger with increased current density.

In this work, a number of n-type Si (100) substrates were fabricated into a few micrometers of porous Si substrate using EC etching at different etching parameters. Detailed experiment will be provided in Chapter 4. Later, GaN layer will be deposited onto the porous Si/Si substrate.

2.5 Growth of GaN on porous Si/Si substrate.

In few decades ago, extensive works had been done to investigate the potential of porous Si towards improving GaN growth. The high uniformity and density of

porous Si are highly desirable to achieve the purpose. The following sections will discuss the role of porous Si as an alternative method for reducing the impact of lattice mismatch and progress in the GaN on porous Si/Si substrate will be reviewed.

2.5.1. Main role of porous Si/Si substrate for GaN growth.

It has been reported that a high quality GaN layer can be grown on porous Si/Si substrate as the impact of large difference in lattice arrangement and thermal expansion coefficient between both materials can be accommodated by the porous structure [62]. Figure 2.6 shows the possible lattice arrangement in the GaN layer grown on porous Si/Si substrate. The created pores on Si substrate reduced the large difference in atomic arrangement between GaN and Si materials. As a result, the GaN layer tends to follow and match the atomic arrangement in porous Si template and good quality of GaN layer could be expected. To the best of our knowledge, the critical thickness for a uniform GaN layer is not well established since it strongly depends on the size of the pores.

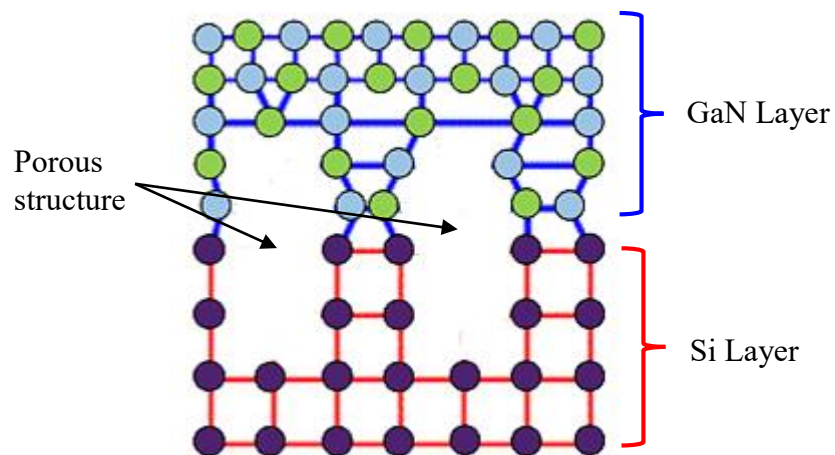


Figure 2.6: Illustration of atomic arrangement in GaN layer on porous Si substrate as the defects propagation in the GaN layer was minimized by the pores structure.

2.5.2 Progress in the growth of GaN on porous Si/Si substrate.

Throughout literature, the effect of Si porosity on the GaN growth is less investigated. Therefore, it is hard to confirm that how different porosity could influence the GaN overgrown layer. This work will conduct the investigation and details will be given in Chapter 4 and Chapter 5. It is suggested that the properties of GaN is dependent on the type of the porosity of the Si/Si substrate.

So far, most of the GaN layers were grown on the p-type porous Si/Si substrate using various techniques like metal organic chemical vapour deposition (MOCVD) and molecular beam epitaxy (MBE) [62-65]. This is because p-type porous Si is very easy to be fabricated. However, the etching process is hard to be controlled and therefore irregular pores and distribution are produced [66]. The irregularity in shape and distribution of the pores will result in poor GaN layer. Matoussi et. al. [63] and Cheng et.al [64] demonstrated the growth of GaN on p-type porous Si/Si substrate using MOVPE. Both of them revealed the formation of cracks on the GaN surface but the crystalline quality is comparable with the GaN growth on non-porous Si substrate. It implies that the potential of p-type porous Si is still limited.

Unlike p-type Si substrate, the fabrication of porous Si on n-type substrate is more promising and controllable since it contains minority carrier of hole concentration. The accumulation of holes on the surface can be controlled by external illumination and therefore effective etching activity can be expected [67]. It seems that n-type Si may have better prospect to improve the porous Si in the field of GaN technology. However, the growth of GaN on n-type porous Si/Si substrate is less demonstrated and therefore will be performed here.

2.5.3 Growth of GaN on porous Si/Si substrate using cost-effective technique

Molecular beam epitaxy (MBE) [7, 62] and metal organic chemical vapour deposition (MOCVD) [63-65] are well-known techniques in GaN epitaxy. These techniques promote excellent interface and surface morphology and being conducted in high purity system [68]. MBE is generally favourable for growing thin epitaxial layer because of its lowest growth rate and excellent thickness monitoring [68]. Meanwhile, MOCVD is more desirable for mass production growth due to easy configurability for scaling up wafer sizes and high uniformity across wafer-to-wafer [69].

Despite of the great advantages of both systems, they are identified as a complex system and require expensive running costs and high maintenance. Alternatively, radio-frequency (RF) sputtering is simpler and inexpensive technique to grow GaN as compared to MBE and MOCVD. The growth of GaN layer by RF sputtering is normally operated in a mixture of nitrogen (N_2) and argon (Ar) gases. It involves the collisions of high energetic ion to the target, which leads to the ejection of atoms and subsequently sputtered to the substrates. Detailed explanation on the principle of operation of the system will be given in Chapter 3.

In general, GaN grown by RF sputtering is always expected in the form of amorphous structure [8-9, 70-71]. At the growth pressure around 10^{-2} mbar, the formation of amorphous structure of GaN layer on Si (100) can easily happen [8]. To minimize the structure, Miyazaki and his team [9] proposed lower growth pressure to achieve better GaN layer. From their observations, it is suggested that the growth pressure of 10^{-4} mbar can reduce the amorphous structure and the GaN layer appears in a specific direction of growth. Similar evidence was also reported by Li et.al [72]

of which the GaN layer is preferably grown in a specific direction. These findings, consequently boost the interest of growing GaN using RF sputtering.

In contrast, electron beam (e-beam) evaporator is another simpler and low-cost technique to grow thin film materials like GaN. Unlike RF sputtering, e-beam evaporator utilizes the bombardment of high energetic electron on GaN source that subsequently heated-up and produces vapour that drifted to the substrate surface. Detailed explanation will be provided in Chapter 3. The unique properties of this system lies on its highly controllable growth rate, which can achieve from 1 nm/min up to 100 000 nm/minutes [73]. Nevertheless, the growth of GaN using e-beam evaporator is not popular among the nitride growth scientists due to its poor morphological structure and the overgrown layer can easily peel-off from the substrate.

To the best of our knowledge, the growth of GaN on Si (100) using e-beam evaporator has only been demonstrated by Chaudhari et.al. [10]. Their work focused on the direct growth of GaN on Si (100) using different temperature. Nonetheless, the grown GaN is in polycrystalline structure. The growth of GaN on porous Si has never been demonstrated by e-beam evaporator and very least by RF sputtering. Despite of their limitation in producing GaN layer with good crystalline properties, post-annealing treatment could be a way to ameliorate the GaN properties. Review on annealing GaN is given below.

2.6 Annealing treatment as a strategy to improve GaN properties.

Post-annealing treatment is one of the best way to improve the quality of the GaN layer. Generally, annealing treatment enables to make the surface morphology, crystalline quality and optical properties to be better. The applied heat allows the

atoms inside the GaN to re-crystallize and form into well-orderly structure, hence reduce defect densities. Several published works have been reviewed on the effect of annealing treatment as an effort to improve GaN properties [74-78]. Note that, the annealing temperature plays the key contribution in the process.

Zhang et.al [74] revealed that the minimum temperature of 600°C is required to decompose the ammonia (NH₃) gas into nitrogen active species (N), which could reduce the non-stoichiometric surface of the treated GaN sample. However, the crystalline quality of the GaN layer will degrade if the temperature is too high due to thermal decomposition, where the GaN re-evaporate out from the surface [76-77]. For example, Hong-Di et.al [76] and Cheng et.al [77] discovered that the crystalline quality of the GaN layer was degraded when the annealing temperature is above 1000°C. This subsequently results in the formation of defects on the surface of the GaN. Throughout literature, the optimum temperature for the annealing treatment was found to be ~950°C, as reported by [77-78]. One should be aware that the optimum annealing temperature will differ in different experiments. Therefore, the optimum annealing temperature for our sample will be investigated using a conventional 3-zone furnace.

2.7 Summary

Basic properties of the GaN material were briefly discussed and the potential substrates for GaN growth were reviewed. Since this thesis focuses on growing GaN layer on porous Si/Si substrate, therefore reports on the Si etching method, the GaN growth technique and thermal annealing as the way to improve the quality of the GaN layers were discussed. In this work, we aim at producing high quality GaN layer grown directly onto the porous Si/Si substrate through the techniques of RF sputtering and e-beam evaporator.